PAPER • OPEN ACCESS

# RFX-mod2 diagnostic capability enhancements for the exploration of multi-magnetic-configurations

To cite this article: L. Carraro *et al* 2024 *Nucl. Fusion* **64** 076032

OPEN ACCESS
IOP Publishing | International Atomic Energy Agency
Nuclear Fusion
Nucl. Fusion **64** (2024) 076032 (11pp)
https://doi.org/10.1088/1741-4326/ad490a

# RFX-mod2 diagnostic capability enhancements for the exploration of multi-magnetic-configurations

**L. Carraro[1,2], M. Zuin[1,2], D. Abate[1], P. Agostinetti[1,2], M. Agostini[1,2,*], D. Aprile[1], M. Barbisan[2], A. Belpane[1], G. Berton[1], M. Bonotto[1], M. Brombin[1,2], R. Cavazzana[1], L. Cinnirella[1,5], S. Ciufo[1,5], G. Croci[2,6], L. Cordaro[1], F. D'Isa[1], S. Dal Bello[1], A. Dal Molin[2], G. De Masi[1,2], G. Emma[1,5], M. Fadone[2], A. Fassina[1,2], D. Fiorucci[1,3], P. Franz[1], L. Grando[1,2], F. Guiotto[1,5], M. La Matina[1], G. Marchiori[1,2], N. Marconato[1,4], I. Mario[1], L. Marrelli[1,2], R. Milazzo[1], S. Molisani[1,5], M. Moresco[1], A. Muraro[2], E. Perelli Cippo[2], S. Peruzzo[2], P. Porcu[1,5], N. Pomaro[1], M.E. Puiatti[1], O. Putignano[2], D. Rigamonti[2], A. Rigoni Garola[1], A. Rizzolo[1], F. Ruffini[1,5], P. Scarin[1], S. Spagnolo[1,2], M. Spolaore[1,2], C. Taliercio[1,2], M. Tardocchi[2], D. Terranova[1,2], M. Ugoletti[2], M. Valisa[1,2], N. Vianello[1,2] and B. Zaniol[1]**

[1] Consorzio RFX (CNR, ENEA, INFN, Università di Padova, Acciaierie Venete SpA), C.so Stati Uniti 4, 35127 Padova, Italy
[2] Institute for Plasma Science and Technology, CNR, Italy
[3] Fusion and Nuclear Safety Department, ENEA, C. R. Frascati (Rome), Rome, Italy
[4] Department of Industrial Engineering, University of Padova, Padova, Italy
[5] CRF—University of Padova, Padova, Italy
[6] Dipartimento di Fisica 'G. Occhialini', University of Milano-Bicocca, Milano, Italy

E-mail: matteo.zuin@igi.cnr.it

Received 19 January 2024, revised 11 April 2024
Accepted for publication 9 May 2024
Published 4 June 2024

**Abstract**

The RFX-mod2 device, the upgraded version of the previous RFX-mod with a modified magnetic boundary, is presently under realization and will start to be operated in 2025. Significant upgrades of the diagnostic capabilities have been proposed and are under development. These include a largely increased number of in-vessel magnetic and electrostatic sensors, a new fast reciprocating manipulator for the exploration of the edge plasma in a wide range of experimental conditions, the improved Thomson scattering and soft x-ray diagnostics system for a detailed determination of the behavior of the electron temperature profile, new dedicated systems for the space and time resolved analysis of x-ray spectra and neutron rate, a reflectometric diagnostic for real-time determination of plasma position, two diagnostics devoted to the imaging of light impurities and influxes behavior along with arrays of halo current sensors. These diagnostic upgrades will be accompanied by a significant effort to improve the control of the electron density and of the impurity influxes by means of proper treatment of plasma facing components with in-vessel fixed electrodes distributed over the first

* Author to whom any correspondence should be addressed.

wall. The described advancements will allow a deeper understanding of physics phenomena in the wide variety of magnetic configurations, including the tokamak, the reversed-field pinch and the Ultra-low q, which can be produced in RFX-mod2 thanks to its flexibility and unique MHD control capabilities.

Keywords: reversed-field pinch, diagnostic, tokamak, helical equilibrium, H-mode

(Some figures may appear in colour only in the online journal)

## 1. Introduction

The RFX-mod2 device [1, 2], the upgraded version of RFX-mod, is planned to start operation in 2025 with a wide range of improvements both in terms of magnetic boundary and diagnostic capabilities. The enhancement of the copper shell plasma proximity, defined as b/a, where b and a are the minor radius of the innermost shell surface and the plasma, which in RFX-mod2 is reduced to 1.04 from being 1.1 in RFX-mod, is expected to significantly improve its passive stabilizing properties. This main modification, along with unique control capability due to the advanced MHD modes feedback system made of 192 independently driven saddle coils and the flexibility of the power supply and shaping coil systems, will open a wider range of experimental conditions in various magnetic configurations, including the reversed-field pinch (RFP), the tokamak and the Ultralow-q (ULq).

Thanks to the modified passive structures, RFX-mod2 is predicted by modelling [3] to exhibit, when operated as a RFP, reduced error fields and reduced MHD modes amplitude. This will give access to operational scenarios characterized by spontaneous mode rotation at significantly higher plasma current (from around 100 kA to >600 kA [4]) and mitigation of plasma wall interaction. Compared to those observed in RFX-mod, helically shaped equilibria in RFX-mod2, which characterize RFP plasmas with low dissipation at high plasma current levels [5, 6], are predicted to be associated with lower level of magnetic perturbation and a higher ratio between dominant and secondary modes. This will result in improved confinement properties associated to more stationary and resilient internal transport barriers.

In addition to RFP, in RFX-mod2 it will be possible to produce both circular and shaped tokamak plasmas, and in particular to explore a variety of single and double null configurations, including the negative triangularity and the low-q ($q(a) < 2$) regimes. Transitions to H-mode can be induced by active modification of the edge radial electric field with an insertable polarized electrode. In this experimental condition, ELM mitigation strategies, based on a wide range of applied magnetic perturbations, can be investigated.

The RFP and the tokamak are characterized by plasma phenomena with largely different spectral properties in terms of typical dominant frequencies and wavelengths on the poloidal, toroidal and radial directions. With the aim of getting larger and more detailed (in space and time) information on the physics quantities both in the core and the edge plasmas in all magnetic configurations, strong effort has been put to improve and extend the diagnostics capabilities, including magnetic field, electron and ion temperature, plasma density, flow and electrostatic potential, neutron and x-ray production, impurity behaviour and halo current measurements. The paper describes the main diagnostic improvements, some of them presently being in the realization phase, some others in the design phase.

## 2. Diagnostic upgrades

### 2.1. Magnetic measurements

As mentioned in the previous section, the spectrum of magnetic configurations producible in RFX-mod2 requires a unique diagnostic capability for the detection of equilibrium and perturbation plasma quantities with a wide range of characteristic time and space scales. This, coupled with the requirements from the sophisticated feedback control algorithms developed for the exploitation of the complex MHD active coil system, suggested a significant improvement of the integrated set of distributed electromagnetic sensors in RFX-mod2 with respect to RFX-mod, with the aim of precisely characterizing also fast magnetic transient phenomena [7]. Since in the new experiment configuration all electromagnetic sensors have been moved inside the vacuum vessel, the signal bandwidth of pick-up coils, previously limited at 1 kHz because of the filtering of the vessel, is increased to 250 kHz.

The local sensors for MHD perturbation are organized in three basic sets, as shown in figures 1 and 2.

Two sets of equally-spaced $B_r$ saddles and $B_t$ pick-up coils, made of $8 \times 72$ (along the poloidal and the toroidal directions, respectively) probes each, are aimed at improving full toroidal 3D reconstruction [8] with magnetic perturbation $n \leqslant 36$; $m = 0, \pm 1, \pm 2$ for the RFP configuration. A third set combines two arrays of 14 by 6 three-axis pick-ups; this has been designed with a focus on the tokamak and Ultra low-q operation, and is organized in a staggered configuration in order to allow reconstructions and detection of poloidal MHD features with mode number up to $m \leqslant 14$. The use of three-axis sensors has the additional advantage of offering the possiblity of compensating for slight probe misalignement.

The distribution of the $B_t$, $B_r$ (saddle coils) and three-axis probes are shown in figure 1, where also a picture of one of the latter is present.

For the acquisition of the foreseen total of 1730 magnetic measurement channels, a system based on a modular bespoke 12 channel DAQ board has been realized. It is based on a high resolution 20 bit, 1 MSamples $s^{-1}$ ADC, galvanically isolated, coupled with an FPGA which performs the numerical

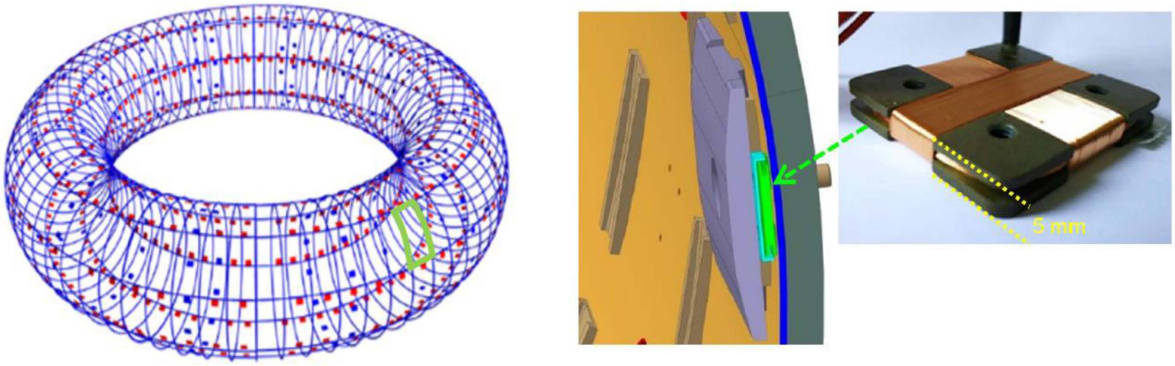


**Figure 1.** On the left, distribution of in-vessel magnetic probe arrays: saddle $B_r$ coils (blue lines, one of them being highlighted with a thick green line), $B_t$ probes (red dots) and three-axis probes (blue dots), along the RFX-mod2 torus; on the right, picture of one three-axis probe and location of installation behind a graphite tile.

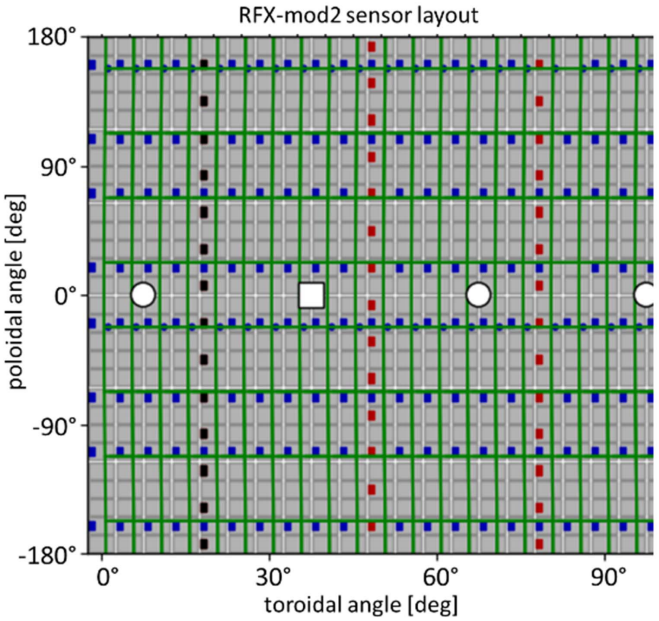


**Figure 2.** Scheme of sensor distribution on the rectified torus map. Radial saddle coil (green lines), toroidal field pickup (blue square), three-axis pick-up (red square), Langmuir probe (round blue), plasma facing tiles in gray. The origin of the poloidal angle is on the outer equatorial plane, with positive values pointing upwards.

integration. The board provides simultaneous high speed transient recording locally and data streaming at reduced sampling rate (up to 20 kSamples $s^{-1}$) for real-time plasma control. This architecture allows a significant cost and space reduction (up to 576 channel can be hosted on each single rack cabinet), and a much more robust noise immunity with respect to the traditional analog integrators architecture, with two separate channel for direct and integrated signals [9].

Moreover, a set of two poloidal arrays of 12 halo sensors mounted on a complete poloidal array of first wall tiles, along with two-axis pick-up coils mounted on the extrenal side of the shell to measure induced currents [10], will allow to test the prediction of electromagnetic modelling on the sideway forces during fast transients in tokamak plasmas, a relevant topic for larger devices such as ITER.


**Figure 3.** Graphite first wall tile with inserted a five-pin electrostatic probe and, on the right, design of the probe.

### 2.2. *Electrostatic sensors system*

RFX-mod2 first wall will be equipped with poloidal and toroidal arrays of electrostatic probes, measuring plasma density and temperature, plasma potential, particle and energy fluxes and floating potential fluctuations. Two toroidal arrays of 71 probes each (one on the high field side and one on the low field side), along with four poloidal arrays (1 of 28, 1 of 36 and 2 of 17 elements) will be installed. Such a large amount of sensors is needed to better characterize the phenomena observed in the RFP, where toroidally localized bulging due to many modes phase locking can induce localized plasma-wall interaction phenomena at high electron density [11] and the self-organized single-axis state, which emerge at high plasma current levels, are found to induce significant modulation of the edge electrostatic turbulence even at small scales (of the order of few cm). Moreover, as mentioned, RFX-mod2 is planned to be operated in a variety of shaped tokamak configurations (circular, single null, double null), where the position of X-point will be moved along the poloidal direction. The high number of probes will allow a detailed reconstruction of the dynamics of the SOL and of the X-point edge plasma region.

In figure 2, a map of the distribution of the various (magnetic and electrostatic) sensors for a toroidal section of the RFX-mod2 is given.

Three different kinds of probe configurations will be installed: single Langmuir probes, five-pin balanced triple probes (an example is shown in figure 3) and ball-pen probes. The expected frequency bandwidth for the acquisisition of the electrostatic measurements is up to 2 MHz, while the power supplies for probes will be equipped with arc-protection

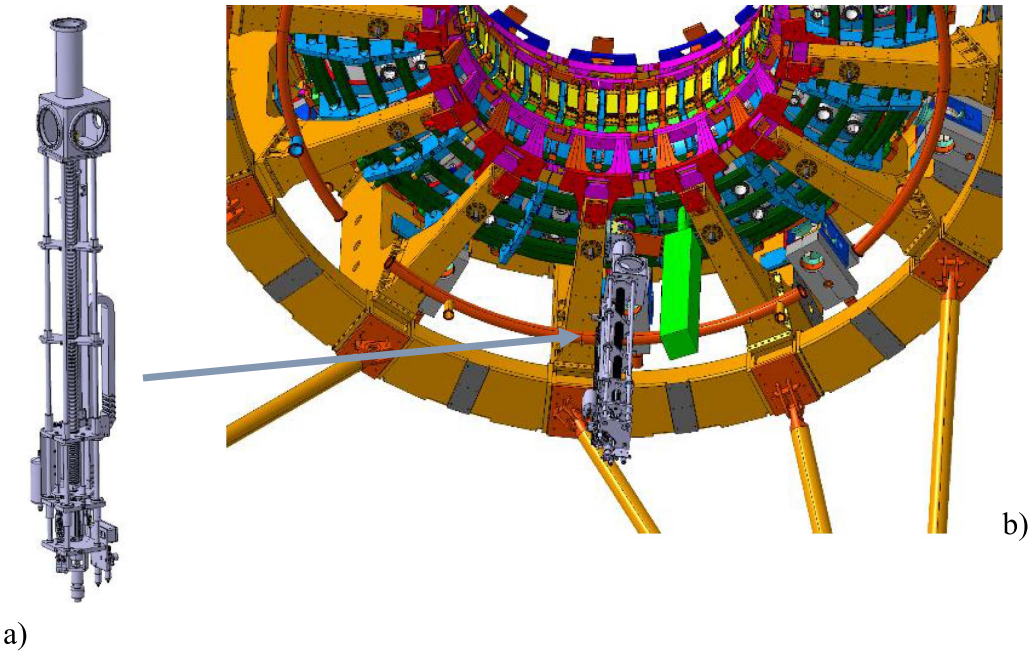


**Figure 4.** (*a*) Design of the fast reciprocating manipulator (FaRM); (*b*) FaRM installation location on the bottom of the RFX-mod2 device.

systems. The design of the probes takes inspiration from the models successfully installed on RFX-mod, which allows the removal of tiles in case of damage, by means of the remote handling manipulator.

### 2.3. Fast reciprocating manipulator(FaRM)

A FaRM for probes to be radially inserted from the bottom side of the machine (see figure 4) has been designed in order to explore the edge plasma in a wide range of plasma conditions including the high plasma current (2 MA) RFP regime, which was not accessible to the insertable probes in RFX-mod due to excessive thermal loads.

The manipulator will host a variety of electro-magnetic sensors for the detection of various plasma parameters (electron density, $n_e$, electron temperature, $T_e$, plasma potential, $V_p$, and magnetic field, $B$) and a detailed analysis of turbulent phenomena. The probes will likely include a combination of high frequency Hall sensors in a cluster distribution for a detailed reconstruction of the magnetic field profiles and, through the curl of the magnetic field itself, of the edge plasma current components in RFP equilibria.

The manipulator will combine a 1500 mm slow transition and a 100 mm fast stroke by means of a pneumatic piston with 2 electric valves. The predicted operation times are 50 ms for insertion and extraction, while the typical time spent in its innermost location will be set between 50 and 200 ms ($v_{max} = 2$ m s$^{-1}$; $a_{max} = 150$ m s$^{-2}$).

### 2.4. High frequency magnetic probes and ion cyclotron emission diagnostic

A set of small three-axis high frequency (up to 10 MHz) magnetic coils ($7\times7\times7$ mm$^3$) will be installed in fixed positions in RFX-mod2 with the aim of characterizing quasi-coherent modes found to emerge from the magnetic spectrum in RFP discharges. A total of 27 probes will be distributed along the toroidal and poloidal locations in order to detect the dispersion properties of modes with wavelengths of the order of the ion-Larmor radius (mainly microtearing modes induced by strong edge pressure gradients, with characteristic poloidal and toroidal mode numbers up to 20 and 300, respectively [12, 13]) as well as long wavelength Alfvén eigenmodes observed and predicted to be destabilized during reconnection phenomena [14, 15]. The probes will be installed inside three boron-nitride cases located in three distinct poloidal positions (on the top and the bottom of the machine and on the outer midplane) in one toroidal position, directly facing the plasma in order to reduce shielding from conductive materials. Each case, placed 1 cm radially outward with respect to the first wall tiles surface, will house 9 probes at a mutual distance of 20 mm along the poloidal and toroidal directions in a symmetric orthogonal cross configuration.

Additional single loop antennas for very high frequency (of the order of few GHz) electromagnetic analysis will be installed and the collected signals fast digitized to study the spectral properties, both in terms of wave polarization and associated wavelenghts, of ion cyclotron emission harmonics for the investigation of fast ion behavior and confinement and for whistler wave detection, as already done in large tokamaks (see for example [16, 17]).

Moreover, a set of high frequency probes, measuring the fluctuations of the poloidal magnetic field component only will be installed behind the graphite tiles as those shown in figure 1. The coils are made of a reduced number of turns with respect to those presented in section 2.1 in order to guarantee a frequency bandwidth up to 2.5 MHz. They will be distributed on a 14-probes full poloidal array and on two partial toroidal arrays of

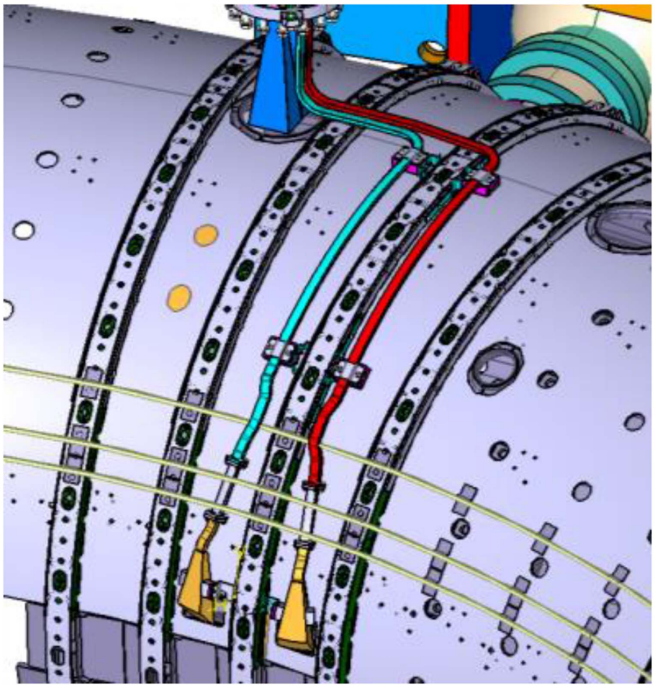

**Figure 5.** Layout of the HFS plasma position relectometer antennas (in yellow) in the RFX-mod2 device.

11 probes each, at two distinct poloidal positions 180 degrees apart, covering almost 50 degress of the toroidal angle.

### 2.5. Reflectometric diagnostics

RFX-mod2 is planned to be the test bed for an innovative technique for plasma position determination in tokamak plasmas, also proposed for DEMO, based on detailed reflectometric measurements, with distributed antennas along the poloidal direction.

The RFX-mod2 plasma position reflectometer (PPR) will be composed by four ultrafast K band units (18–26 GHz) installed at the same toroidal section: two on the equatorial plane (from inner High Field Side and outer Low Field Side respectively) and two at the vertical top/bottom ports [18].

The very limited physical space imposed different design choices: standard elongated pyramidal horns will be installed in top/bottom/LFS accesses; conversely, in the HFS region a hog-horn reflector concept has been developed and an in-vessel fundamental waveguide routing will bring the signal from the top port (see figure 5).

The design of the HFS antennas, based on the hog-horn scheme, has been preliminary studied with the help of a COMSOL model. Different layouts have been compared in order to minimize the presence of secondary lobes and maximize the antenna gain. The complex geometry suggested the use of the metal additive manufacturing technique. To validate the manufacturing process of the antennas different bench tests were developed to assess the performance of the system.

From the application point of view, the RFX-mod2 PPR will allow the investigation of the horizontal and, for the first time on a fusion experiment, vertical plasma position control based on reflectometric measurements. In particular, whilst density and magnetic field distribution may affect the measurement range of the reflectometric system, the typical operational parameters expected for RFX-mod2 are such that a single K-band in X-mode can cover the position of the separatrix in different magnetic configurations. This test will shed light on different issues linked to the use of a more sophisticated PPR scheme on fusion reactors like DEMO.

Moreover, following the good results obtained on RFX-mod [19], that demonstrated for the first time the reflectometry capabilities on RFP plasmas, the existing ultrafast narrow band (in the Ka frequency range) profile reconstruction reflectometer will undergo a significant modification. A O-mode, multi band (K, Ka and U) reflectometric system driven by an upgraded control circuit will replace the outdated diagnostic components. A heterodyne detection is also under consideration with respect to the present homodyne scheme. This will allow to reconstruct the edge density profile with a high time resolution (5–10 $\mu$s) in the density range expected in RFX-mod2.

### 2.6. MANTIS

The polycromator MANTIS (Multispectral Advanced Narrowband Tokamak Imaging System [20]) was designed and installed for the first time on the TCV tokamak [21, 22], from the modification of the multi-spectral imaging diagnostic (MSI) [23]. This diagnostic, planned to be installed in RFX-mod2, allows the simultaneous imaging of several atomic emission lines from a common sight view. It aims at providing a quantitative measurement of plasma parameters in 2D at high spatial and temporal resolution.

In the diagnostic system, the light is collected by a bundle of coherent fiber optics and focalized by a lens. A bundle of coherent fiber optic is an assembly of multiple optical fibers arranged in a specific geometric pattern to maintain the spatial coherence of light transmitted through the bundle. Each optical fiber in the bundle preserves the relative spatial relationships of the light rays, allowing for coherent imaging and transmission of optical signals.

The bundle is 1.5 m long, with size 5.4 mm $\times$ 7.2 mm, as the sensor of each camera. An objective with 12 mm focal length on the side looking at the plasma would provide an image of about 40° along the toroidal direction.

The resulting image is reflected by the field mirror to the relay lens, the interference filter and then the camera behind it. The filter transmits the desired wavelength then detected by the camera. All the other wavelengths are reflected by the filter itself to the following field mirror, allowing the propagation to the next channel, where another wavelength is selected by the interference filter in a cascade process. The conceptual layout is shown in figure 6 for a 10-channel design.

Since at each step the image is filtered and reflected to the next channel, vignetting, aberration and absorption must be minimized, while conserving a high efficiency and good spectral selectivity (1 nm bandwidth).

This diagnostic will observe the visible emission of the plasma near the first wall, with the goal of characterizing the

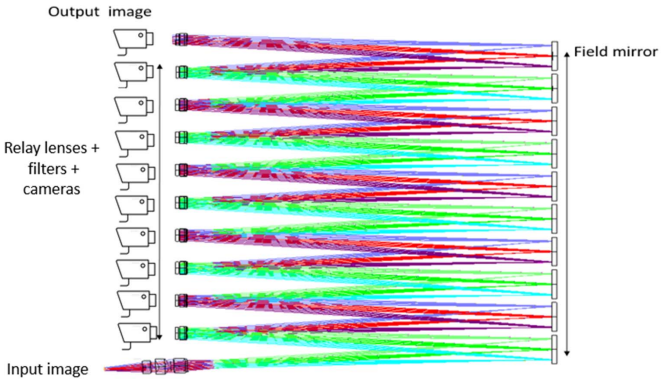


**Figure 6.** Work principle of a 10-channel MANTIS diagnostic.

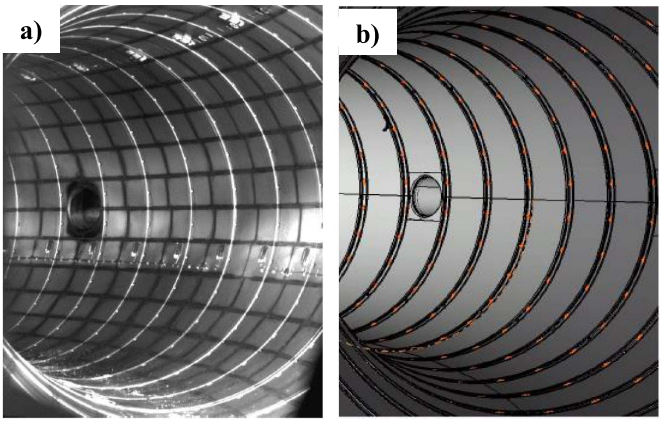


**Figure 7.** Camera spatial calibration technique test: experimental image of the inner vessel (without graphite tiles) of RFX-mod2 (*a*) compared with the CAD design (*b*).

plasma edge of RFX-mod2 to resolve the steep temperature and density gradients, as well as to study the impurity distributions. Calibrated images of the intensity of different emission lines can be used in collisional radiation models, allowing local plasma parameters such as temperature and density to be obtained, with high spatial and temporal resolution. For these purposes, 4 He and 3 H emission lines are selected, allowing the estimation of the electron temperature and density. The 2D distribution of the low ionized stages of B, C, O impurities can be reconstructed from the measurement. Thanks to the versatility of this diagnostics, two different designs are being studied: a single system consisting of 10 channels or 2 devices of 6 channels each; in the last solution, a beam splitter would split the light coming from the fiber bundle, producing two images into the two systems. The latter is smaller and with a reduced number of reflections, easily preserving the quality of the images and allowing flexible positioning in different accesses along the torus.

Regarding the spatial calibration of the camera, in order to project the 3D coordinates onto the 2D image of the camera, the pinhole camera model and the camera calibration technique described in [24] will be implemented, identifiing the geometrical transformation that links each camera pixel to the 3D world. Both intrinsic (such as the focal length) and extrinsic parameters (describing the orientation of the camera), and the equation of each line of sight will be identified.

The technique has been succesfully tested experimentally, as shown in figure 7. The intrinsic parameters have been obtained by taking several images of a black and white plane chessboard with known dimension, as described in [20]; the extrinsic parameters have been obtained by taking the image of inner surface of RFX-mod2 vacuum vessel. By comparing the 2D image obtained with the CAD design of the vessel, the rotation matrix $R$ and the translation vector $t$ are obtained., and finally the line of sight of each camera pixels is uniquely defined.

### *2.7. Light impurity tomography (LIT)*

RFX-mod2 will be equipped with a set of spectroscopic diagnostics for the study and the characterisation of the 3D plasma wall interaction. In fact, the edge of RFP plasmas is intrinsically 3D due to the presence of magnetic modes, as shown in [25, 26]. In particular, the LIT is a diagnostic designed for studying the poloidal distribution of the plasma wall interaction, a missing information in the old RFX-mod experiment. LIT will observe the poloidal distribution of the emission of neutral hydrogen or of impurities that are present in the edge region, like carbon and oxygen, with the main goal of comparing it with the magnetic structure of the plasma boundary, and to do this it has to be capable of distinguishing among $m = 0, 1, 2$ modes.

The diagnostic consists of seven cameras, installed in seven different portholes around the poloidal direction, with changeable interference filters. The seven cameras observe line-integrated signals, and the 2D map of the emissivity of the specific ion species selected by the interferential filter is obtained with a tomographic inversion. An example of layout of cameras and LoSs (presently in the definition phase) is shown in figure 8. In order to obtain a good tomographic inversion of $m = 2$ modes with seven lines of sight, any symmetry in the arrangement of the lines of sight (LoSs) has to be avoided. To do this, some mirrors will be installed inside some of the portholes, so that some LoSs will be reflected and symmetry will be minimized.

The layout of the seven cameras with optics is identical, and shown in figure 9. A commercial $f = 24$ mm objective collects the emission of the plasma; then, a $f = 85$ mm objective collimates the light perpendicularly to the interference filter. The incidence angle has to be as low as possible, compatible with a narrow bandpass (1–2 nm) in order to select only the desired line and to avoid wavelength contamination. Then, a second $f = 85$ mm objective focuses the image into the camera sensor.

The selected camera is a USB3 Basler acA1920-155 $\mu$m, with square pixels with size 5.86 $\mu$m, and a sensor of $11.3 \times 7.1$ mm$^2$. With this optical setup, each camera observes a region at 0.5 m of about $220 \times 140$ mm$^2$.

In additiion, an upgraded visible camera system (VCS) [27] will measure the CI emission at 909.5 nm to complete the information obtained by the LIT. A total of seven cameras will be installed in 4 toroidal locations: three of these ports

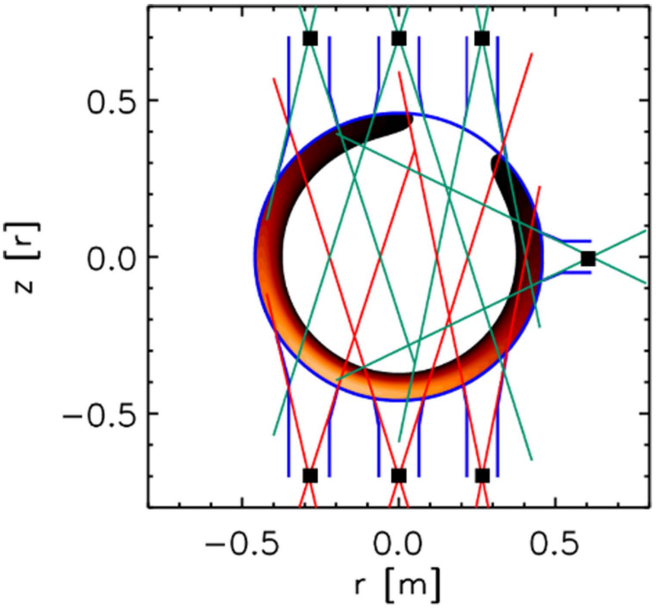


**Figure 8.** Scheme of the LIT diagnostic. Color lines represent the cone of view of the seven cameras. As an example, the edge emission is here shown with a $m = 1$ periodicity.

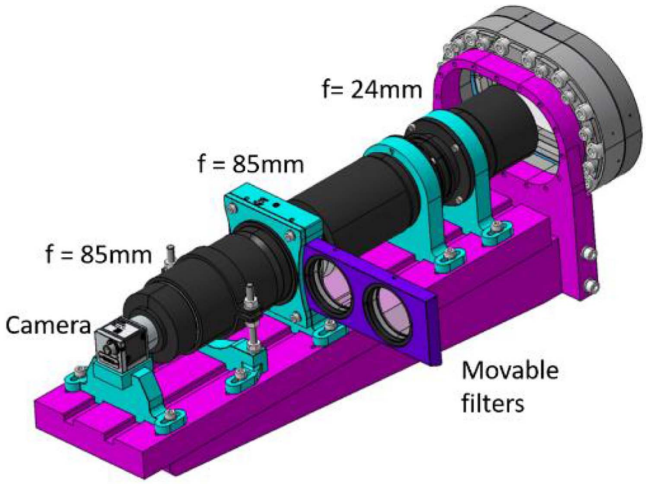


**Figure 9.** Layout of the optical head of one camera. On the right there is the porthole with the window. The camera is on the left side. The light is collected by a $f = 24$ mm objective; a first $f = 85$ mm objective will allow a perpendicular incidence of the light onto the filter; the second $f = 85$ mm objective focuses the light on the camera sensor.

will host two cameras (as shown in figure 10) looking at two opposite toroidal directions, providing a 2D image of 70% of the outboard first wall surface. This system is designed so that the cameras are installed inside portholes in ambient atmosphere, at about 100 mm from the plasma. This solution guarantees a large cone of view with a very simple optics. As a drawback, in this region, a magnetic field of about 500 mT is expected (at a 2 MA plasma current level), mostly produced by the plasma current itself; this can cause problems on the electronic board of the camera. The Basler acA720–520 $\mu$m camera, with 720 × 540 square pixels with 6.9 $\mu$m side, and

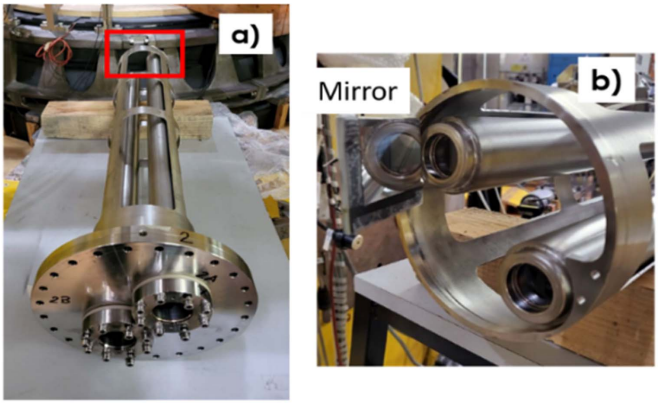


**Figure 10.** Camera support structure for two cameras ($a$). The zoom of the head (red rectangle in ($a$)) is shown in ($b$). The two tubes at atmospheric pressure will contain one camera each. In front of them, in vacuum two metallic mirror (only one mounted in the picture) will allow to see in the two toroidal directions.

maximum frame rate of 525 fps at full resolution, has been experimentally verified to withstand a magnetic field up to 850 mT. Cameras will be equipped with commercial objectives with $f = 12$ mm.

This system, however, will give images of the first wall only at a single line, the CI. To overcome this limitation, one camera can be removed and replaced with a coherent fibre bundle, which carries the image on a MANTIS system.

The edge characterization is completed by means of the Thermal Helium Beam and Gas Puffing imaging diagnostics, already present in RFX-mod. The former provides the edge $T_e$ and $n_e$ radial profiles exploiting the He line intensity ratio technique, including photon re-absorption [28, 29]. The second measures the edge fluctuations related to turbulence [30].

### *2.8. Soft-x-ray and Thomson diagnostics for electron temperature profile measurement*

A higher repetition rate Thomson scattering (TS) system and a strengthened Soft x-ray diagnostic based on the double filter (DF) technique, are designed for a better understanding of the dynamics of the electron temperature profile with particular focus on thermal barrier formation [3].

This aspect is of particular relevance in RFX-mod2 as purer and longer lasting helical magnetic RFP equilibria (SH), associated with improved energy confinement regimes, are expected to occur in high plasma current conditions, due to combined effects of passive and active MHD stabilization [3].

In RFX-mod the main TS diagnostics featured a laser entering radially through an aperture on the vacuum vessel, travelling on the equatorial plane, and dumped on the torus inner equator [31]. The space allocated for the beam dump was sufficient to install a number of carbon plates to ensure months of safe dump-operation. With the foreseen change in RFX-mod2 plasma boundary and first wall, the space allocated for the laser dump is drastically reduced, because of the changes in the vacuum vessel and in the first wall. Tests and calculations on optical layouts and suitable optical components are

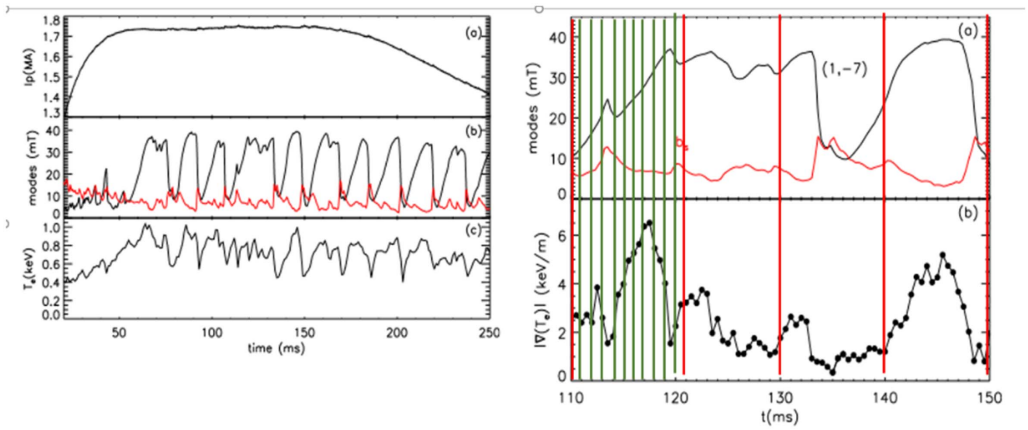


**Figure 11.** Left panels, time traces of a typical high plasma current RFP discharge in RFX-mod. From the top: plasma current, dominant $m = 1/n = 7$ mode amplitude (black) and secondary modes amplitude (red), electron temperature $T_e$. Right panels: at the top, time behavior of mode amplitude (dominant and secondary modes in black and red, respectively) and, at the bottom, time behavior of the edge temperature gradient; vertical red lines represent the timing of the existing Thomson scattering system and green lines the one to be produced in RFX-mod2, with a starting time triggered by a given threshold of the dominant mode.

ongoing to assess the feasibility of a double passage layout, where the laser is not dumped but back reflected on the inner equator [32]. The double laser passage will amplify the signal level, crucial for diagnostic operation in low density RFP and tokamak discharges.

A manipulator to install/remove the internal dump or mirror, if the double passage will result feasible, has been designed and is under construction. Together with the manipulator, the entire optical support frame has been modified to simplify maintenance operations, in particular to allow operation without breaking the machine vacuum.

Moreover, a new Nd:Yag laser able to produce a burst train of more than 10 pulses with repetition rate of the order of 1 KHz will be acquired. Such system will be coupled to the already available TS diagnostic Nd:Yag laser, to better follow the $T_e$ profile time evolution during the setting-up of the SH and the back transition to the so-called multiple helicity state characterized by many modes with comparable amplitude, associated to magnetic reconnection phenomena. To the purpose, the laser burst will be triggered by the dominant mode amplitude: as an example in figure 11 the desired timing scheme of the TS laser pulses applied to an old RFX-mod discharge is shown, the green vertical lines representing the time of the new laser pulses, the red one the existing 100 Hz laser pulses.

The obtained $T_e$ profiles will be complemented by and compared with the results of 2D $T_e$ maps obtained with the expanded DF SXR diagnostic. In the new SXR DF diagnostic for RFX-mod2 the $T_e$ measurements will be available on 58 LOSs: 39 lLOSs distributed on the three top vertical accesses of the SXR tomography, as shown in green in figures 12, and 19 LOSs on the horizontal access, which were already available in RFX-mod (in blue in the figure).

An improvement of the time resolution of the bolometry, measuring from the three bottom vertical accesses of figure 11, from 500 Hz to 2 KHz is also foreseen. The ion temperature dynamics during the SH phase, a key ingredient for the confinement evaluation, will be measured with the refurbished 50 keV, 100 kW Diagnostic Neutral Beam Injector [33, 34] and with an upgraded compact Neutral Particle Analyzer, thus covering a gap of RFX-mod, where information about ion dynamics where rather limited. An optimized pumping system will be installed to significantly minimize the DNBI beam losses caused by charge exchange before the beam enters the plasma. These losses previously affected the RFX-mod DNBI

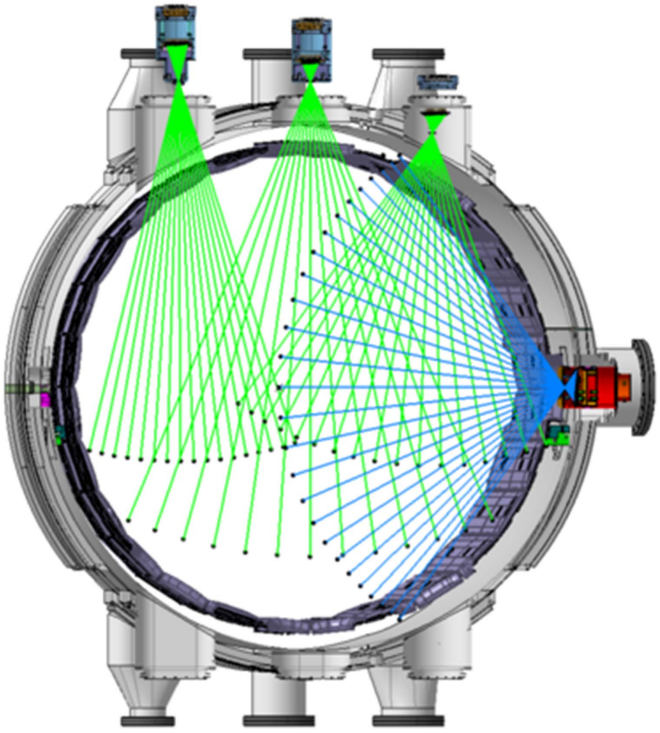

**Figure 12.** Lines of sight of the new double filter SXR diagnostic system (in green). In blue, the original system already present in RFX-mod.

system. Additionally, the design phase is underway for Charge Exchange Recombination Spectroscopy and Motional Stark Effect diagnostics for the RFP discharges of RFX-mod2.

### *2.9. Neutron and gamma-ray diagnostics*

A neutron camera system based on an array of inorganic scintillators that exploits the $^{35}$Cl(n,p)$^{35}$S nuclear reaction to allow neutron measurements resolved in space, energy, and time is presently being developed.

The system will consist of two chambers vertically looking at different plasma regions, the core and the plasma edge. Monte Carlo simulation codes are used to determine the number of lines of sight, the materials, and the geometrical properties of the collimators that better suits the application at RFX-mod2. The detection will be based on the scintillation light induced by charged products released in the $^{35}$Cl(n,p)$^{35}$S nuclear reactions. These charged products produce a univocal peak dependent on the neutrons kinetic energy plus the reaction Q-value (0.615 MeV). Therefore, by measuring the broadening of the peak, it is possible to obtain information about the ion temperature of the reactants.

Two scintillation materials that contain $^{35}$Cl have been proposed: CLYC ($Cs_2LiYCl_6$:Ce) and $LaCl_3$:Ce. CLYC scintillators have already been used to measure fusion neutrons in [35], showing excellent spectroscopic and Pulse Shape Discrimination (PSD) capabilities to separate the neutrons from the gamma-ray background. The main drawback is the slow pulse decay time of the CLYC crystal (of a few $\mu$s), which can limit the maximum achievable counting rate. On the other hand, $LaCl_3$:Ce scintillators have a higher rate capability thanks to a pulse decay time of $\sim$30 ns, but they have a limited literature, and their PSD capability needs to be investigated. Regardless of the type of crystal that will be chosen, each scintillator will be coupled to a Silicon Photomultiplier to avoid gain shifts due to the presence of the strong magnetic field. The proposed neutron camera system will be able to perform measurements of the neutron rate and the energy spectrum in each line of sight, making it possible to measure the fusion power (after a specific characterization) and the temperature of supra-thermal ions that are believed to mostly produce 2.5 MeV neutrons at RFX-mod2.

### *2.10. Gas electron multiplier (GEM) soft-x-ray detection system*

The RFX-mod2 device is especially well-suited for investigating the potential effects of applied magnetic perturbations on the confinement of runaway electrons (REs) in tokamak plasmas. This research is essential to comprehend how REs are generated and to find strategies to minimize their harmful consequences, such as damages to the vacuum vessel and the plasma facing components.

One of the most commonly employed diagnostic techniques for identifying REs in fusion devices is the detection of Bremsstrahlung emission. When REs interact with ions within the plasma, they undergo a significant deceleration, leading them to emit x-rays at higher energies compared to the x-rays produced by the bulk plasma. As a result, the x-rays generated by REs through Bremsstrahlung emission can fall within the energy range 1–20 keV, which is the optimal detection range for soft x-rays using GEM detectors [36]. This energy range is of particular interest also in RFP plasmas, as electron acceleration has been observed to occur up to around 20 keV during magnetic reconnection phenomena [37]. Two GEM detectors for RFX-mod2 equipped with three GEM foils and an anode segmented into rectangular pads are presently being developed. A GEM foil is made of a Kapton layer (50 $\mu$m thick) clad on each side with a thin layer of Aluminum and chemically perforated to obtain a high-density matrix of bi-conical holes. The detection is based on the electron multiplication in each GEM foil due to the large electric field within the bi-conical holes. GEM detectors allow to have imaging capability with good spatial resolution ($\sim$ 1 mm) and an energy resolution of $\sim$20% at 6 KeV. They are characterized by a high-rate capability (up to $\sim$1 MHz mm$^{-2}$), a temporal resolution of $\sim$10 $\mu$s, good optical flexibility, good radiation hardness and insensitivity to background gamma rays and neutrons. In RFX-mod2, the installation is foreseen of two GEM detectors with crossing lines of sight (see figure 13) in order to attempt a 3D tomographic reconstruction of the SXR emission spectra coming from the plasma.

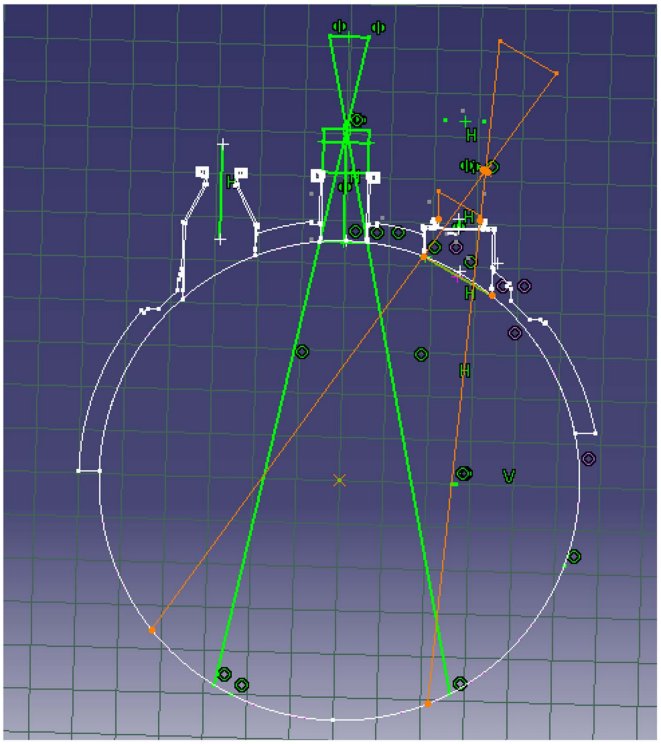

**Figure 13.** Preliminary layout of the GEM cones of sight in RFX-mod2.

## 3. First wall cleaning system

A set of fixed in-vessel electrodes for the generation of helium (and/or hydrogen) glow discharge cleaning (GDC) plasmas on an inter-shot basis has been designed with the aim to improve

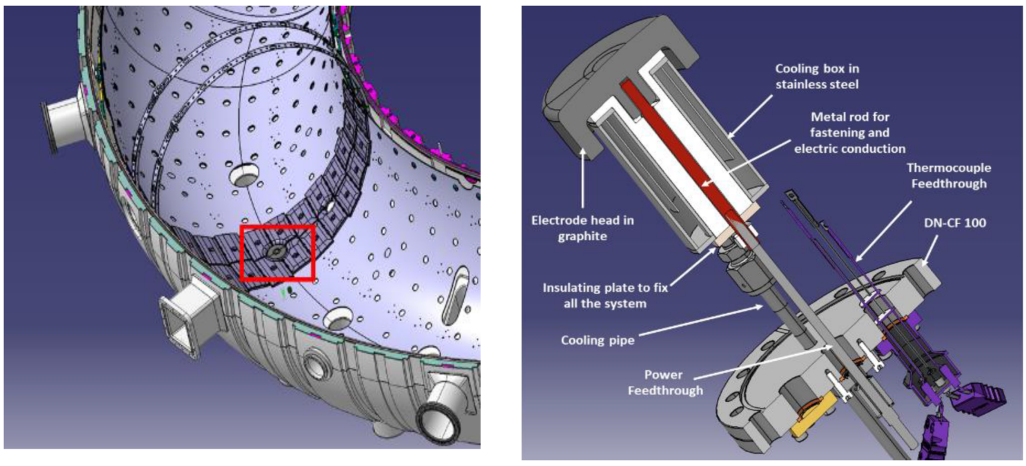


**Figure 14.** On the left, position of the fixed electrode to be installed in RFX-mod2; on the right the complete final design of one of the electrodes.

the reproducibility of the first wall condition, which has been proven to strongly influence the RFP plasma performance, in particular at high current levels.

This system will be composed of 8 electrodes distributed in various toroidal and poloidal positions to get a rather uniform GDC plasma. The electrodes are mainly made of a graphite head, in the same radial position as that of the graphite tiles of the first wall, and are designed to withstand 1 kW of total power in a steady state GDC mode and 37 MW $m^{-2}$ for 0.1 s, which is the estimated power expected to be locally deposited by the main plasma in case RFX-mod2 enters in a locked mode condition in a 2 MA discharge (see figure 14, where the installation position and the design of one of the electrodes are reported).

The new electrodes system will not replace the original one of RFX-mod, made of two insertable electrodes. The original electrodes will be kept in use for the application of Helium discharges for first wall Boronization, which typically implies possible material deposition on the electrode surface. The use of movable and retractable electrodes makes maintenance a significanlty easier process.

Moreover, the pulsed-discharge cleaning technique, based on short-lasting, relatively high-power toroidal plasma current transients, is designed for first wall heating. The deriving improved reproducibility of the first wall condition should give the possibility to apply real-time electron density control methods even in the largest plasma current RFP operations, when the ohmic input power can exceed 60 MW.

## 4. Summary

RFX-mod2 will start operation in 2025, after relevant modifications of the magnetic boundary, which are predicted to enhance confinement properties in a variety of magnetic configurations. This, thanks to flexibility of the power supplies, of the shaping coils and of the advanced MHD control systems, spans from the RFP to the circular and shaped tokamak even in very-low q equilibria. With the aim to characterize the wide range of plasma phenomena expected to have largely different time and space scales, relevant upgrades of the diagnostics capabilities are under realization.

These include the significant improvement of the number of magnetic measurements (mostly installed in-vessel for better time resolution) and of the electrostatic sensors, a new reciprocating manipulator, a novel reflectometric determination of plasma position for real-time control and new systems for the space resolved analysis of impurities and influxes for a fine determination of the plasma edge properties. The behaviour of electron temperature profiles, strongly affected by MHD dynamics in the RFP, will be highly resolved in space and time thanks to the improvement of TS and Soft-x-ray diagnostics. Novel neutron diagnostics will shed light on the anomalous ion heating phenomena which spontaneously enhance DD fusion rate in RFP. The enhanced diagnostic capabilities will be accompanied by an expected relevant improvement of electron density control, thanks to upgraded first wall conditioning systems.

## Acknowledgments

This work has been carried out within the framework of Italian National Recovery and Resilience Plan (NRRP), funded by the European Union—NextGenerationEU (Mission 4, Component 2, Investment 3.1—Area ESFRI Energy—Call for tender No. 3264 of 28-12-2021 of Italian University and Research Ministry (MUR), Project ID IR0000007, MUR Concession Decree No. 243 del 04/08/2022, CUP B53C22003070006, ‘NEFERTARI—New Equipment for Fusion Experimental Research and Technological Advancements with Rfx Infrastructure’). Views and opinions expressed are however those of the author(s) only and do not necessarily reflect those of the European Union or the European Commission. Neither the European Union nor the European Commission can be held responsible for them.

This work has received support by the Royal Society (UK) and the Consiglio Nazionale delle Ricerche (Italy) through the International Exchange Cost Share scheme/Joint

Bilateral Agremment project Multi scale electrostatic energisation of plasmas: comparison of collective processes in laboratory and space (award numbers IEC\\R2\\222050 and SAC.AD002.043.021).

The authors would like to thank for valuable technical and administrative support in the development of the project all the colleagues from Consorzio RFX.

## ORCID iDs

M. Zuin https://orcid.org/0000-0002-0282-2978
D. Abate https://orcid.org/0000-0002-0331-3454
P. Agostinetti https://orcid.org/0000-0003-2103-7630
M. Agostini https://orcid.org/0000-0002-3823-1002
M. Barbisan https://orcid.org/0000-0002-4065-3861
A. Belpane https://orcid.org/0009-0009-9054-1364
M. Bonotto https://orcid.org/0000-0001-9147-7506
G. Croci https://orcid.org/0000-0001-9720-7232
L. Cordaro https://orcid.org/0000-0002-8068-5307
A. Dal Molin https://orcid.org/0000-0003-0471-1718
G. De Masi https://orcid.org/0000-0002-5283-5478
L. Marrelli https://orcid.org/0000-0001-5370-080X
S. Spagnolo https://orcid.org/0000-0002-2187-8141
D. Terranova https://orcid.org/0000-0001-9339-283X
M. Ugoletti https://orcid.org/0000-0002-7498-0780
N. Vianello https://orcid.org/0000-0003-4401-5346

## References

[1] Marrelli L. *et al* (RFX-Mod Team) 2019 *Nucl. Fusion* **59** 076027
[2] Peruzzo S. *et al* 2023 *Fusion Eng. Des.* **194** 113890
[3] Terranova D. *et al* RFX-mod2 as flexible device for reversed-field-pinch and low-field tokamak research *29th Fusion Energy Conf. (FEC 2023)* (*London, UK, 16–21 October 2023*) p CN–2136 (available at: www.iaea.org/events/fec2023)
[4] Zuin M. *et al* 2017 *Nucl. Fusion* **57** 102012
[5] Lorenzini R. *et al* 2009 *Nat. Phys.* **5** 570
[6] Piovesan P. *et al* (the RFX-mod Team) 2009 *Nucl. Fusion* **49** 085036
[7] Marconato N., Cavazzana R., Bettini P. and Rigoni A. 2020 *Sensors* **20** 2929
[8] Zanca P. and Terranova D. 2004 *Plasma Phys. Control. Fusion* **46** 1115–41
[9] Manduchi G. *et al* 2021 *Fusion Eng. Des.* **167** 112329
[10] Bonotto M., Cavazzana R., Abate D., Aprile D. and Berton G. 2022 *IEEE Trans. Plasma Sci.* **50** 4096–101
[11] Agostini M. and Scarin P. 2020 *Plasma Phys. Control. Fusion* **62** 025009
[12] Zuin M. *et al* 2013 *Phys. Rev. Lett.* **110** 055002
[13] Predebon I., Sattin F., Veranda M., Bonfiglio D. and Cappello S. 2010 *Phys. Rev. Lett.* **105** 195001
[14] Spagnolo S., Zuin M., Auriemma F., Cavazzana R., Martines E., Spolaore M. and Vianello N. 2011 *Nucl. Fusion* **51** 083038
[15] Kryzhanovskyy A., Bonfiglio D., Cappello S., Veranda M. and Zuin M. 2022 *Nucl. Fusion* **62** 086019
[16] Spong D. *et al* 2018 *Phys. Rev. Lett.* **120** 155002
[17] Liu L.N. *et al* 2019 *Rev. Sci. Instrum.* **90** 063504
[18] De Masi G., Cavazzana R., Abate D., Bernardi M., Marchiori G., Moresco M., Tiso A. and Peruzzo S. 2021 *J. Instrum.* **17** C01071
[19] De Masi G., Cavazzana R., Fassina A., Martines E., Momo B. and Moresco M. 2011 *Nucl. Fusion* **51** 053016
[20] Perek A. *et al* 2021 *Nucl. Mater. Energy* **26** 100858
[21] Vijvers W.A. *et al* 2017 *J. Instrum.* **12** C12058
[22] Perek A. *et al* 2019 *Rev. Sci. Instrum.* **90** 123514
[23] Mumgaard R.T., Scott S.D. and Khoury M. 2016 *Rev. Sci. Instrum.* **87** 11E527
[24] Zhang Z. 2000 *IEEE Trans. Pattern Anal. Mach. Intell.* **22** 1330–4
[25] Scarin P., Agostini M., Spizzo G., Veranda M. and Zanca P. (the RFX-Mod Team) 2019 *Nucl. Fusion* **59** 086008
[26] Agostini M. *et al* (RFX-mod Team) 2017 *Nucl. Fusion* **57** 076033
[27] Valisa M. *et al* 2001 *J. Nucl. Mater.* **290–293** 980
[28] Kajita S. and Ohno N. 2011 *Rev. Sci. Instrum.* **82** 023501
[29] Agostini M., Scarin P., Milazzo R., Cervaro V. and Ghiraldelli R. 2020 *Rev. Sci. Instrum.* **91** 113503–1
[30] Agostini M., Scarin P., Cavazzana R., Fassina A., Alfier A. and Cervaro V. 2010 *Rev. Sci. Instrum.* **81** 10D715
[31] Alfier A. and Pasqualotto R. 2007 *Rev. Sci. Instrum.* **78** 013505
[32] Fassina A. and Franz P. 2017 *J. Instrum.* **12** C11021
[33] Carraro L., Puiatti M.E., Sattin F., Scarin P. and Valisa M. 1999 *Rev. Sci. Instrum.* **70** 861–4
[34] Korepanov S.A. *et al* 2004 *Rev. Sci. Instrum.* **75** 1829
[35] Rigamonti D. *et al* 2019 *J. Instrum.* **14** C09025
[36] Muraro A. *et al* 2019 *J. Instrum.* **14** C08012
[37] DuBois A.M., Almagri A.F., Anderson J.K., Den Hartog D.J., Lee J.D. and Sarff J.S. 2017 *Phys. Rev. Lett.* **118** 075001